

EBIC mode characterization of transport properties on laser heterostructures

M.J. Romero ^{a,*}, D. Araújo ^a, J.D. Lambkin ^b, R. García ^a

^a *Departamento de Ciencia de los Materiales e I.M. y Q.I., Facultad de Ciencias, Universidad de Cádiz., Apdo. 40, 11510 Puerto Real (Cádiz), Spain*

^b *National Microelectronics Research Centre, University College Cork, Lee Maltings, Prospect Row, Cork, Ireland*

Abstract

A method for the quantitative evaluation of electron-beam-induced current (EBIC) profiles across p–n junctions (normal-collector configuration) is presented. The procedure consists of firstly estimating the extent of electron–hole (e–h) pair generation by Monte Carlo calculations. Secondly, the steady-state diffusion equation is applied to minority carriers in each differential volume to evaluate the minority carrier collection probability. The model is then used to investigate ($\lambda = 1.3 \mu\text{m}$) InGaAsP/InP double bulk heterostructure lasers. From the comparison of experimental and calculated linescans, the minority carrier diffusion length and surface recombination velocity are evaluated to be $L = 0.52 \mu\text{m}$ and $S/D = 1 \times 10^5 \text{ cm}^{-1}$ at n-side and $L = 0.87 \mu\text{m}$ and $S/D = 5 \times 10^4 \text{ cm}^{-1}$ at p-side. © 1997 Elsevier Science S.A.

Keywords: Double bulk heterostructure lasers; Electron-beam-induced current; Transport properties

1. Introduction

Investigations of transport properties in heteroepitaxial structures have attracted significant interest not only as consequence of the fascinating physics related to quantum size effects, but also because of the necessity to fully characterize optoelectronic and microelectronic production devices. In general, mobilities are estimated from Hall-effect measurements [1,2], while recombination lifetimes are determined from time-of-flight (TOF) experiments [3–5]. To determine diffusion lengths, therefore, such complementary techniques are necessary. The electron-beam-induced current (EBIC) mode of the scanning electron microscope (SEM) allows us to evaluate the minority carrier diffusion length and the surface recombination velocity in the sub-micron scale [6–11]. The EBIC detection principle is based on the presence of local electric fields, such as that formed by a p–n junction, a Schottky contact or even crystal defects. In most cases, transport properties cannot be

straightforwardly quantified and a method to model EBIC linescans is required. The principal reasons for such a difficulty are the extent of electron–hole (e–h) pair generation due to electron beam excitation and/or surface recombination processes, perturbing the minority carriers transport. To overcome such difficulties, we present in this contribution a procedure that takes into account both influences on EBIC profiles, which thereby allows us to determine the bulk minority carriers diffusion lengths. The proposed algorithms also allow the estimation of the surface recombination velocity. The extended e–h generation is estimated, at a specified electron beam energy, from the Monte Carlo method. Both depth and lateral e–h distributions have been compared with the first reliable experimental measurements [12]. The next step consists of applying the steady-state diffusion equation to generated carriers in each differential volume for each point of the EBIC linescan. This procedure is then subsequently applied to extract the bulk minority carrier diffusion length and the surface recombination velocity in normal-collector geometry across the p–n junction in InGaAsP/InP double bulk heterostructure lasers (DBHL).

* Corresponding author.

2. Experimental technique

The EBIC linescan profiles are collected from InGaAsP/InP ($\lambda = 1.3 \mu\text{m}$) DHBLs used as p–n junctions. The laser was grown by metal–organic vapor phase epitaxy (MOVPE) on an n-doped (Si, $1 \times 10^{18} \text{ cm}^{-3}$) InP substrate at 900 K and nominal atmospheric pressure (III–V ratio: 100). The structure is presented schematically in Fig. 1. The undoped active region consists of a 100 nm InGaAsP ($\lambda = 1.3 \mu\text{m}$) layer sandwiched between two InGaAsP ($\lambda = 1.15 \mu\text{m}$) layers of 50 nm. The cladding layers are composed of 1.5 μm p-doped (Zn, $8 \times 10^{17} \text{ cm}^{-3}$) and 1.0 μm n-doped (Si, $2 \times 10^{18} \text{ cm}^{-3}$) InP. The DHBLs are capped by 100 nm of $4 \times 10^{18} \text{ cm}^{-3}$ p-doped $\text{In}_{0.53}\text{Ga}_{0.47}\text{As}$.

The EBIC linescans were measured from a freshly cleaved (110) face perpendicular to the epilayers in the [001] direction, that is to say, in the normal-collector configuration (geometry of Fig. 2). The current induced by electron beam excitation was measured using a Matelect ISM-5A amplifier and Matelect IU-1 interface. The EBIC experimental set-up was installed on a JEOL-820SM scanning electron microscope.

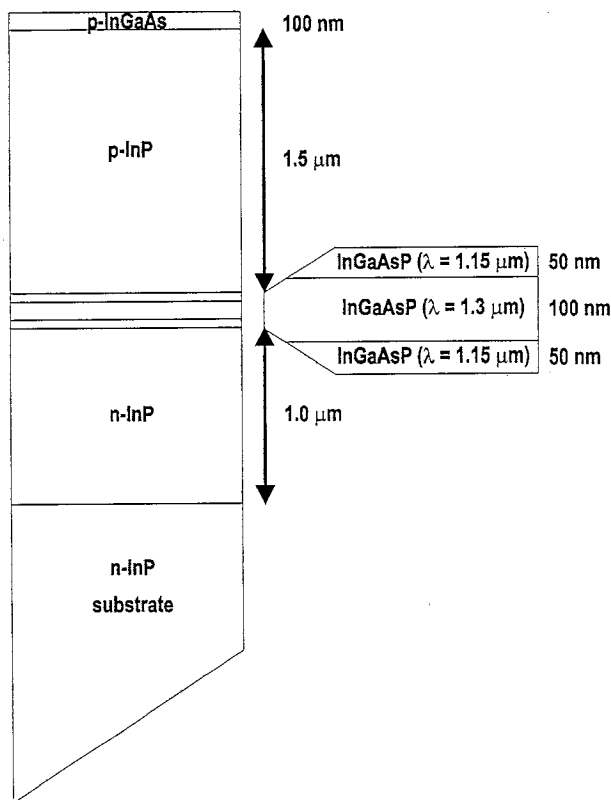


Fig. 1. Schematic diagram of ($\lambda = 1.3 \mu\text{m}$) InGaAsP/InP double bulk heterostructure laser.

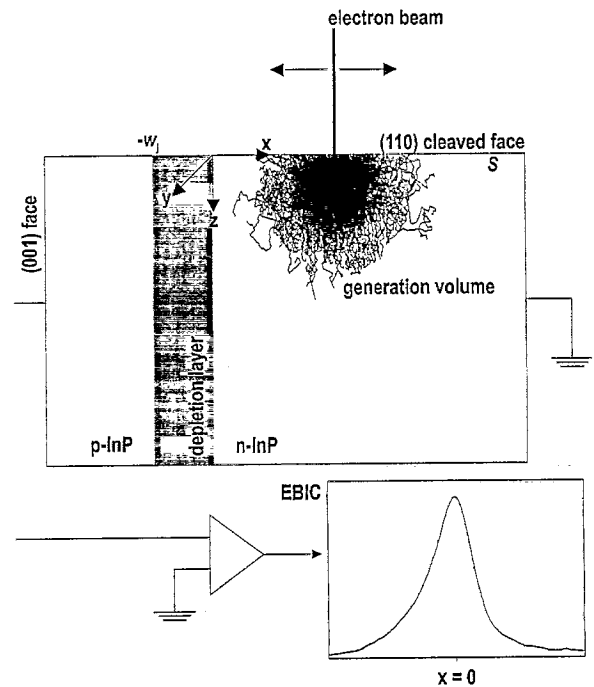


Fig. 2. Schematic representation of the normal-collector geometry used for EBIC profile measurements, performed along the [001] direction. The coordinates system (x, y, z), the depletion layer width (w_d) associated coordinate and the surface recombination velocity S close to (110) face are shown.

3. Results and discussion

During the electron beam excitation, when e–h pairs are generated beneath electron-beam point of impact, excess carrier diffusion occurs. At low-level injection, the induced current is controlled by minority carriers diffusion. Those that reach the space-charge region (SCR) drift to the other side by the p–n junction's electrical field, inhibiting their recombination and subsequently collected as a current. The recorded EBIC profile, therefore, shows a maximum at the depletion layer region. Outside the depletion region, physics phenomena are described by the steady-state equation,

$$D\nabla^2 p(r) - \frac{1}{\tau} p(r) + g(r) = 0, \quad (1)$$

where $g(r)$ describes the e–h generation at $r(x, y, z)$ coordinates, $p(r)$ is the minority carrier density, D is the diffusivity related to mobility μ by the Einstein relation $D = \mu(k_B T/e)$, and τ is the effective minority carrier lifetime that includes the radiative, non-radiative lifetimes and also the surface recombination process. D and τ are related through the minority carrier diffusion length L , $D = L^2/\tau$. The diffusion problem in normal-collector geometry may be reduced to a two-dimensional problem, as a consequence of EBIC not being dependent on its y -coordinate. Therefore, $g(\bar{x}, \bar{z})$ and

$p(\tilde{x}, \tilde{z})$ are expressed by ($\tilde{x}, \tilde{y}, \tilde{z}$ are the generation coordinates):

$$g(\tilde{x}, \tilde{z}) = \int_{-\infty}^{+\infty} g(\tilde{x}, \tilde{y}, \tilde{z}) d\tilde{y}$$

$$p(x, z) = \int_{-\infty}^{+\infty} p(x, y, z) dy. \quad (2)$$

The boundary conditions are defined by the normal-collection set-up, that is: (a) the junction is assumed as a perfect collector, i.e., no recombination processes occur across the p–n junction; and (b) the surface is characterized by its recombination velocity S ,

$$D \frac{\partial p(x, z)}{\partial z} \Big|_{z=0} = Sp(x, z) \Big|_{z=0}. \quad (3)$$

The collected EBIC profile, $I_{\text{EBIC}}(x)$, may then be defined as:

$$I_{\text{EBIC}}(x) = \int_0^{+\infty} p(x, z) dz$$

$$= \int_0^{+\infty} \int_{-\infty}^{+\infty} g(\tilde{x}, \tilde{z}) \varphi(\tilde{x}, \tilde{z}) d\tilde{x} d\tilde{z}, \quad (4)$$

where $\varphi(\tilde{x}, \tilde{z})$ is the minority carrier collection probability when the e–h are generated at (\tilde{x}, \tilde{z}) . From the boundary condition (Eq. (3)) of the steady-state equation, the minority carrier density must be in the form of:

$$p(x, z) = p_{3D}(x, z) \left[1 - \frac{\chi}{1 + \chi} \exp\left(-\frac{z}{L}\right) \right]. \quad (5)$$

We define χ as the ratio of minority carrier diffusion length and surface depletion length ($\chi = S(L/D)$), and $p_{3D}(x, z)$ as the minority carrier density (i.e., the solution of Eq. (1)) in the absence of surface perturbation (the infinite-three-dimensional case):

$$p_{3D}(x, z) = \exp\left(-\frac{d_j}{L_{\text{eff}}}\right) \int_0^{+\infty} \int_{-\infty}^{+\infty} g(\tilde{x}, \tilde{z}) \exp\left(-\frac{z - \tilde{z}}{L}\right) dx dz. \quad (6)$$

In this expression, the first exponential term corresponds to the lateral dependence of the minority carrier density where d_j and L_{eff} are the coordinate related to the junction ($-w_j \leq x \leq 0$) and the minority carrier effective diffusion length, respectively. Hence, $d_j = x$ on the n-side ($x > 0$) and $d_j = -(x + w_j)$ on the p-side ($x < -w_j$). The effective diffusion length is expressed as:

$$L_{\text{eff}} = L \sqrt{1 - \frac{\chi}{1 + \chi} \exp\left(-\frac{\tilde{z}}{L}\right)}, \quad (7)$$

where \tilde{z} , the integrated minority carrier density depth is given by

$$\tilde{z} = \frac{1}{\gamma} \int_0^{+\infty} \int_{-\infty}^{+\infty} zp(x, z) dx dz. \quad (8)$$

The factor γ ensures the normalization of the $p(x, z)$ function. Therefore $I_{\text{EBIC}}(x)$ is fully given by:

$$I_{\text{EBIC}}(x) = \int_0^{+\infty} \exp\left(-\frac{d_j}{L_{\text{eff}}}\right) \left(1 - \frac{\chi}{1 + \chi} \exp\left(-\frac{z}{L}\right) \right) \int_0^{+\infty} \int_{-\infty}^{+\infty} g(\tilde{x}, \tilde{z}) \exp\left(-\frac{z - \tilde{z}}{L}\right) d\tilde{x} d\tilde{z} dz. \quad (9)$$

To take account of the extended e–h generation $g(\tilde{x}, \tilde{z})$, we have developed a Monte Carlo procedure using the modified scattering model of Kanaya et al.¹ as physics background, rather than the more commonly used Rutherford–Bethe model. To compute EBIC linescans, the number of generated e–h pairs $g(\tilde{x}, \tilde{y}, \tilde{z})$ on every scattering event is evaluated. Hence, $g(\tilde{x}, \tilde{y}, \tilde{z}) = [E(i-1) - E(i)]/E_{\text{eh}}$, where $E(i)$ is the i -step electron-beam energy and E_{eh} the energy of an e–h pair generation. Thus, $g(\tilde{x}, \tilde{y}, \tilde{z})$ is reduced to an \tilde{x}, \tilde{z} -dependence by Eq. (2).

Both L and S/D parameters are related by Eqs. (7) and (8). Fig. 3 displays the dependence of L_{eff}/L on S/D for $E_b = 5$ keV. For $\log(S/D) \leq 2$, the ratio $L_{\text{eff}}/L \approx 1$, whereas L_{eff}/L decreases strongly, particularly for large values of L at $\log(S/D) \geq 6$. An evaluation of bulk minority carrier lengths and surface recombination velocity is possible by comparing the simulated and experimental profiles. The magnitude of the S/D ratio is assessed from the linescan shape. Consequently, on the

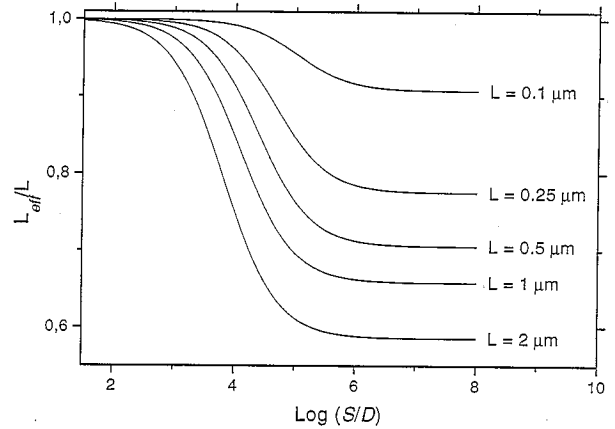


Fig. 3. The L_{eff}/L ratio vs. S/D for different bulk minority carrier diffusion lengths L . The effective diffusion length L_{eff} may be evaluated from the exponential-decay region of the EBIC linescan profiles, or directly from the integrated minority carrier density depth \tilde{z} determination by the Monte Carlo integration subroutine (Eq. (8)). The \tilde{z} values for bulk diffusion lengths displayed on the figure (in the form of (L, \tilde{z}) ; both expressed in μm) are: (0.1, 0.173), (0.25, 0.229), (0.5, 0.344), (1, 0.567) and (2, 0.839).

¹ To be submitted to *Materials Science and Engineering B*.

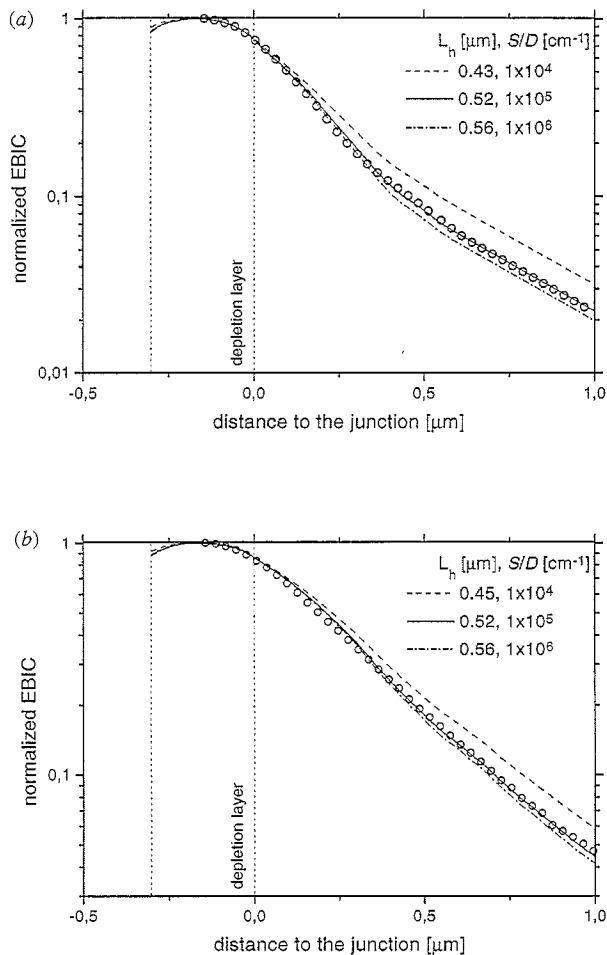


Fig. 4. Experimental EBIC linescans at the n-side of the ($\lambda = 1.3 \mu\text{m}$) InGaAsP/InP DHBL (\circ) and simulated EBIC profiles (—) in the 1×10^4 to $1 \times 10^6 \text{ cm}^{-1}$ S/D range. The effective hole diffusion lengths L_{eff} (corresponding to different L) are equalized to (a) $L_{\text{eff}} = 0.394 \mu\text{m}$ (experimental case) at energy beam $E_b = 5 \text{ keV}$ and (b) $0.415 \mu\text{m}$ at $E_b = 10 \text{ keV}$.

n-side of the DBHL p–n junction, it is rapidly estimated that S/D lies between 10^4 and 10^6 cm^{-1} . We determine the hole effective diffusion length by fitting an exponential-like decay to the experimental EBIC data in the region $x \geq 0.7 \mu\text{m}$. At $E_b = 5 \text{ keV}$ we obtain $L_{\text{eff}} = 0.394 \mu\text{m}$. Then, the simulated EBIC profiles are performed at different S/D (between 10^4 and 10^6 cm^{-1}), using the bulk hole diffusion length values L_h , which gives $L_{\text{eff}} = 0.39 \pm 0.01 \mu\text{m}$, as shown in Fig. 4(a). The closest-fitting simulated profile corresponds to $S/D = 1 \times 10^5 \text{ cm}^{-1}$ and $L_h = 0.52 \mu\text{m}$. These results are in agreement with EBIC linescans at $E_b = 10 \text{ keV}$, dis-

played on Fig. 4(b). The accuracy of the minority carrier bulk diffusion length determination is estimated at $\pm 0.01 \mu\text{m}$. As for the p-side, the minority carrier diffusion length (electrons) results in $L_e = 0.87 \mu\text{m}$ and $S/D = 5 \times 10^4 \text{ cm}^{-1}$.

4. Conclusion

A computational procedure to simulate EBIC across p–n junctions has been proposed. From the extended e–h pair generation dependence on beam energy deduced from Monte Carlo calculations and applying the steady-state diffusion equation to generated e–h pairs in each differential volume, the EBIC linescan is deduced. The bulk diffusion lengths and surface recombination velocities at each junction sides are determined from direct comparison of simulated with experimental profiles.

Acknowledgements

This work was supported by the Comisión Interministerial de Ciencia y Tecnología (CICYT), under MAT94-0538 Project, and by the Junta de Andalucía (Group 6020 PAI). The work was carried out at the Electron Microscopy Division of the University of Cádiz. The authors would like to thank J.-M. Bonard and J.-D. Ganière for useful discussions.

References

- [1] C. Guillemot, M. Baudet, M. Gauneau, A. Regreny and J.A. Portal, *Phys. Rev. B*, **35** (1987) 2779.
- [2] H. Sakaki, T. Noda, K. Hirakawa, M. Tanaka and T. Matsusue, *Appl. Phys. Lett.*, **51** (1987) 1934.
- [3] K. Hattori, T. Mori, H. Okamoto and Y. Hamakawa, *Appl. Phys. Lett.*, **51** (1987) 1259.
- [4] R.A. Höpfel, J. Shah, P.A. Wolff and A.C. Gossard, *Phys. Rev. B*, **37** (1988) 6941.
- [5] H. Hillmer, S. Hansmann, A. Forchel, M. Moroshashi, E. Lopez, H.P. Meier and K. Plogg, *Appl. Phys. Lett.*, **53** (1988) 1937.
- [6] D.B. Wittry and D.F. Kyser, *J. Appl. Phys.*, **36** (1965) 1387.
- [7] D.B. Wittry and D.F. Kyser, *J. Appl. Phys.*, **38** (1976) 375.
- [8] M. Watanabe, G. Actor and H.C. Gatos, *IEEE Trans. Electron. Devices*, **24** (1977) 1172.
- [9] C.J. Wu and D.B. Wittry, *J. Appl. Phys.*, **49** (1978) 2827.
- [10] J.-F. Bresse, *Scanning Electron Microscopy*, **4** (1982) 1487.
- [11] D. Araújo, L. Pavesi, Nguyen Hong Ky, J.-D. Ganière and F.K. Reinhart, *J. Phys. (Paris) IV*, **1** (1991) C6-225.
- [12] J.-M. Bonard, J.-D. Ganière, B. Akamatsu and D. Araújo, *J. Appl. Phys.*, **79** (1996) 8693.